



ÉCOLE POLYTECHNIQUE  
FÉDÉRALE DE LAUSANNE

# Create a Finite Element model of experiment involving cadaveric scapulae

Raphaëlle Peyraud

---

## Semester project

### Supervisors :

Yasmine Boulanaache  
Dr Alexandre Terrier  
Prof Dominique Pioletti

**EPFL**

**Mechanical engineering  
Lausanne, Switzerland**

June 8, 2018

# Abstract

**Hypothesis:** Nowadays, the number of people suffering from shoulder osteoarthritis increases as the population is ageing. An end-stage treatment is the total shoulder arthroplasty (TSA), but it still suffers from a high failure rate in comparison to other joints arthroplasty. To better understand the causes and the mechanisms of this high failure rate, researchers tend to build patient-specific model. To build these models, a workflow composed of different steps has to be carried out. The first step is the segmentation process, which allows to extract the geometry of the patient scapula. Different methods of segmentation are used and two of them were investigated. Indeed, it has been hypothesise that the uncertainty in the segmentation can translate into a larger one in the modelling outputs. The quantification of such errors has never been done. The goal was to estimate the errors between the two segmentation methods, which are, the "manual" and the "semi-automated" ones.

**Methods:** The two segmentation methods are applied on one cadaveric scapula. The manual segmentation is realised thanks to thresholds values and manual adjustments, while for the semi-automated segmentation, the cortical bone is extracted by the use of thresholds values and manual adjustments, but the trabecular bone is obtained by a shrunk of 3mm of the cortical contour segmented manually. Then, each bone geometry obtained were implanted, and a FE model was build for each of them. The exactly same steps were applied to each bone geometry in the steps following the segmentation process, to influence as less as possible the error estimation. The error was estimated by comparing the modelling outputs of both models.

**Results:** The semi-automated segmented bone geometry went through all the steps and the FE outputs were as expected. The manual segmentation suffered from invalid geometries and no proper mesh could have been generated due to the extreme thin cortical thickness in the glenoid cavity. No errors estimation was then performed. It was remarked that the difference of segmented volume between the two methods was important.

**Conclusion:** The semi-automated segmentation process is an easy and fast method to implement. The manual segmentation is extremely time consuming and the build up of the FE model is more challenging, but more accurate. The huge different in segmented volume makes believe that the segmentation process influences the modelling outputs. The comparison of the two methods should be made on more scapulae to drawn global conclusions.

# Contents

<b>Abstract</b>	<b>2</b>
<b>1 Introduction</b>	<b>5</b>
<b>2 Methods</b>	<b>6</b>
2.1 FEM Workflow . . . . .	6
2.2 Segmentation . . . . .	6
2.2.1 Semi-automated segmentation . . . . .	7
2.2.2 Manual segmentation . . . . .	7
2.3 Smoothing . . . . .	8
2.4 Cortical geometry . . . . .	10
2.5 Virtual arthroplasty . . . . .	10
2.5.1 Implant selection and placement . . . . .	10
2.6 Finite element model . . . . .	11
2.6.1 Geometry . . . . .	11
2.6.2 Material properties . . . . .	11
2.6.3 Surface interactions . . . . .	11
2.6.4 Loading hypothesis . . . . .	12
2.6.5 Mesh . . . . .	13
2.6.6 Outputs . . . . .	13
2.7 Statistical analysis . . . . .	13
2.7.1 Methods overview . . . . .	13
2.7.2 Application to this work . . . . .	15
<b>3 Results</b>	<b>15</b>
3.1 Bone . . . . .	15
3.2 Cement . . . . .	18
<b>4 Discussion</b>	<b>18</b>
4.1 Semi-automated segmentation . . . . .	18
4.1.1 Bone . . . . .	18
4.1.2 Cement . . . . .	19
4.2 Manual segmentation . . . . .	20
<b>5 Limitations and further improvements</b>	<b>22</b>
5.1 Manual segmentation workflow . . . . .	22
5.2 Statistical analysis . . . . .	23
5.3 Manual segmentation control . . . . .	23
5.4 Material inhomogeneity . . . . .	24
5.5 Material anisotropy . . . . .	24
5.6 Prosthesis choice and placement . . . . .	24
<b>6 Conclusion</b>	<b>25</b>

# List of Figures

2.1	Workflow showing the steps required to build a FEM and realised a FEA. . . . .	6
2.2	Different bone volume obtained after the segmentation process . . . . .	8
2.3	Differences between the two segmentation method for the trabecular bone (yellow). The same slice on the CT data is selected. . . . .	9
2.4	Differences between the two segmentation method for the trabecular bone (yellow). The same slice on the CT data is selected. . . . .	9
3.1	Relative volume of the bone which undergo Von Mises stress (MPa). . . . .	16
3.2	Relative volume of the bone which undergo octahedral shear strain. . . . .	17
3.3	Contour of the von Mises stress on the semi-automated segmented scapula . . . . .	17
3.4	Relative volume of the cement which undergo minimum principal stress. . . . .	18
3.5	Relative volume of the cement which undergo octahedral shear strain. . . . .	19
4.1	Manually segmented scapula, where highlighted regions are the ones that the pro- gram could not deal with. . . . .	21
4.2	Zoom on the glenoid cavity of the manually segmented scapula, where highlighted regions are the ones that the program could not deal with. . . . .	21
4.3	Cut of the manually segmented scapula parallel to the frontal plane. The delimited closed regions are the cortical and trabecular boundaries. . . . .	22

# 1 Introduction

Osteoarthritis (OA) of the shoulder joint causes pain and reduction of mobility, and particularly affects the elderly. Through the years, there is more and more cases of glenohumeral osteoarthritis since the population is ageing. A treatment for end-stage glenohumeral osteoarthritis is the total shoulder arthroplasty (TSA). Even though the frequency of this surgical procedure increases, but its failure rate is still high compared to the one of hip or knee arthroplasty. The main cause of the failure of a TSA is the glenoid loosening. This leads to a revision surgery which is not without risks. Indeed, the infectious risk is higher for a revision surgery and more over, a revision surgery involves an increase in health costs.

In order to better understand the causes, the mechanisms, and to prevent the failure of a TSA, patient-specific finite element model of the glenoid bone are developed. To build such a model, the bone geometry is needed. The acquisition of the bone geometry is realised thanks to CT (Computed Tomography) data images. CT data are composed of parallel slices of a physical object which are stacked together to form a 3D volume. To extract cortical and trabecular bone separately, segmentation is applied on multiple slices. The segmentation is the process of classifying the voxels in an image into a set of distinct classes. Actually, there exists different methods and ways of segmentation that are being improved in order to spare time and be more accurate. A not exhaustive list can be: thresholding, clustering, Markov random fields models, artificial neural networks, etc[4][3].

The aim of the project is to determine if there is an influence of the segmentation on the final results of the FE simulation. Two different segmentation will be realised, one "manual" and one "semi-automated". In fact, as it has been shown that the geometry and more, the type of bone (trabecular or cortical) plays a big role in the outputs of the simulation[2] [6], it can easily be postulated that if the segmentation method differs, and thus the amount of bone considered as cortical or trabecular varies, the final results will be affected.

The first method called "semi-automated" segmentation will be the one proposed by A. Terrier et al.[2] where the cortical bone thickness of the scapulae was kept constant and equal to 3 mm. The trabecular bone was defined as the rest part. The trabecular bone is obtained through the cortical part which is shrunk. This is why this method is called "semi-automated". The second method that will be used is the "manual" one. Here the trabecular bone will be segmented manually (visually) which means that the observer will decide if a pixel belongs to the trabecular class. The cortical bone will be the rest part of the scapulae. These two methods are both thresholding methods[3][4].

Then the all workflow of the Finite Element model analysis will be realised with one special care. Indeed to be sure to isolate only the difference that could result from the two different techniques of segmentation, the exact same steps must be applied through the softwares for the two methods.

The simulation is realised based on CT data images (CHUV: Department of Orthopaedics and Department of Radiology) of a left cadaveric scapulae (from ScienceCare, Arizona USA). To determine if there is a link between segmentation techniques and simulation outputs, a comparison of the modelling outputs of the two methods is made.

## 2 Methods

### 2.1 FEM Workflow

In order to build a patient-specific model, the workflow illustrated below in the figure 2.1 was applied. As a first step, CT data were obtained from the CHUV. In this case, the CT data were not ones of patients, but of a cadaveric scapula. Then the bone geometry was extracted by a segmentation process. Here, the two segmentation methods were applied both on the same scapula. After that, a virtual arthroplasty was performed. All the parts were assembled and the implant choice and its placement were made at this step. As the assembly was then available, a FEM was build and thanks to that, outputs such as stresses and strains were extracted to realised the comparison and so the error estimation between the two segmentation methods.

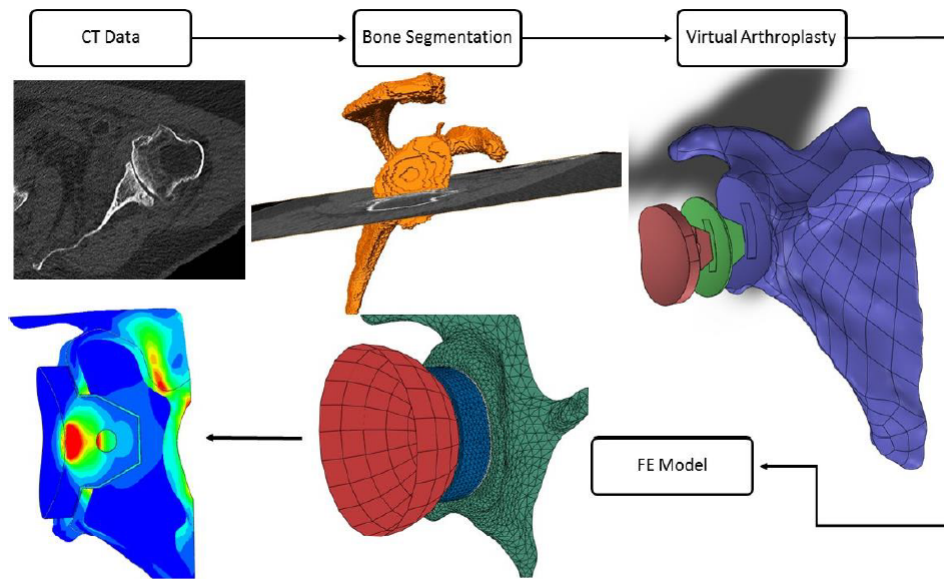


Figure 2.1: Workflow showing the steps required to build a FEM and realised a FEA.

### 2.2 Segmentation

Segmentation of CT images of the scapula is performed by the use of the software Amira 6.2.0<sup>1</sup>. CT images are produced by x-rays imaging technique. In fact, the attenuation coefficient of the material  $\mu$  is measured and the contrast (CT intensity) between the different tissues in the image is due to the differences of this  $\mu$ . Indeed, each material has a proper attenuation coefficient. This coefficient depends among others on the density of the material. So there is a relationship between the grey levels of the CT image and the bone density. Thanks to that, the different types of bones (cortical and trabecular) can be extracted from such images, because cortical and trabecular bone have different density. The CT intensity is measured in absolute terms (CT-number). This number is given in Hounsfield units (HU) [12].

In this project, the model was realised based on a cadaveric scapula. Thus the CT images available were images from the scapula alone. The humerus which is normally present on patient CT images

<sup>1</sup>FEI Visualization Sciences Group, Burlington, Massachusetts, USA.

was missing and the cadaveric scapula was "cleaned". Indeed, there were no muscles attached to the given bone, less fat and surrounding human tissues. That made the segmentation process easier and thus faster because contrast between bone and air (in this case) is greater than contrast between bone and tissues[6].

For the purpose of this project, the segmentation has said before was realised two times on the same scapula but with two different methods. The first method applied, which will be called "semi-automated", is the one used by Terrier et al. [1] where a cortical thickness of 3 mm was considered. The second method, called "manual" is the one where the cortical and the trabecular bone are segmented manually by the user just based on his self assignment of each pixel to each bone category.

In order to gain time doing segmentation (more time consuming step), a threshold in the CT-numbers (HU) was used to help chose if one pixel belongs to either cortical or trabecular bone. The used thresholds used were 300 (HU) for the cortical and 200-300 for the trabecular bone.

### **2.2.1 Semi-automated segmentation**

The cortical bone part of the scapula was segmented based on the thresholds values and manual adjustments were made in order to segment as well as possible this part. A special care was given to the contour of the cortical bone. As the contour was extracted and as it was generated a closed surface, it was filled. This obtained geometry represented the whole scapula.

In order to have a minimum of 3 mm of cortical thickness, the extracted contour (whole scapula) was eroded by 3 mm in each direction. This action was realised by the available function "shrunk" of the software. As one pixel is 0.49 mm long, the contour was shrunk six times. The obtained eroded geometry was taken as the trabecular bone part.

The cortical bone part of 3 mm thickness was obtained by subtraction of the whole contour by the trabecular part. This subtraction was realised in Solidworks<sup>2</sup> and is explained later in the report.

### **2.2.2 Manual segmentation**

The contour of the whole scapula was conserved from the semi-automated method and was reused in this method.

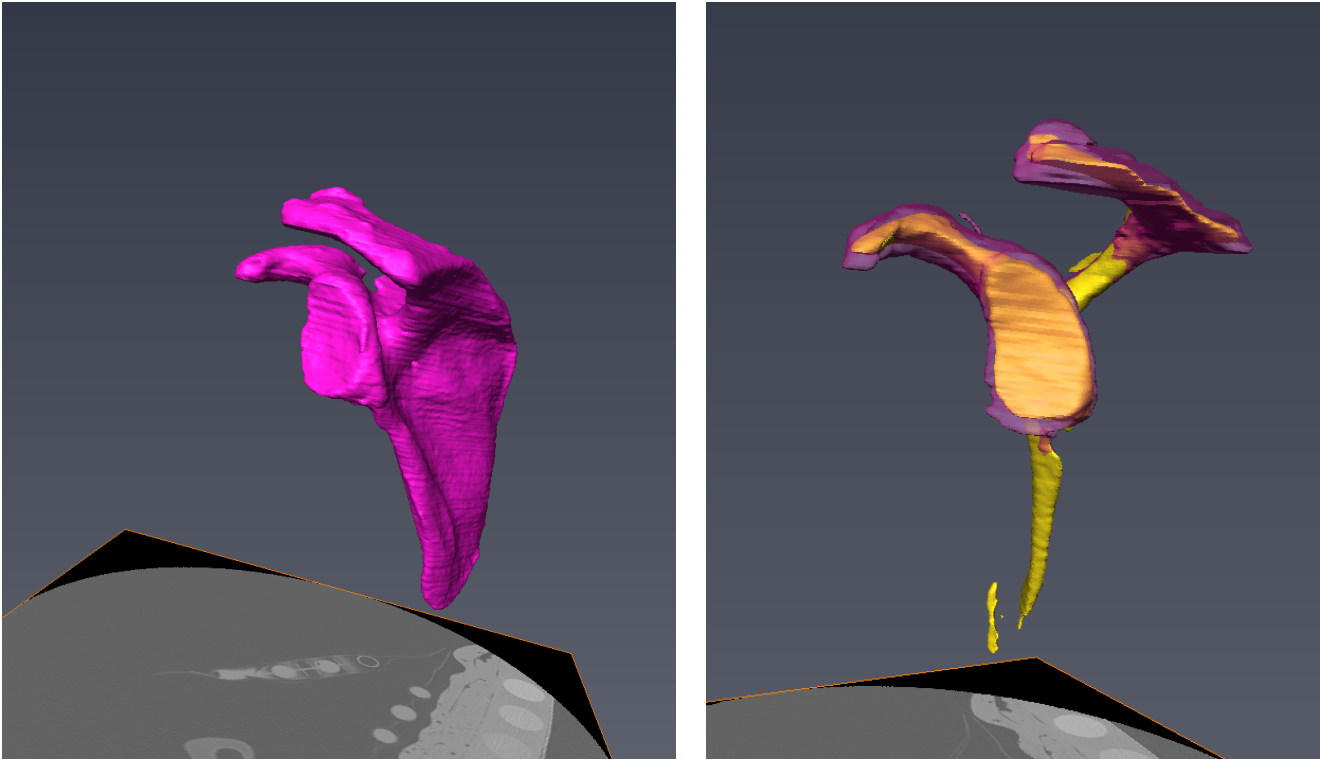
In this method, the trabecular bone part was segmented manually based on the thresholds values and manual adjustments were realised.

The cortical bone part was as before obtained by subtraction of the whole scapula by the trabecular part. Thus in this method, no minimum cortical thickness is ensured.

This method compared to the semi-automated one is more time consuming because the trabecular is segmented manually by the user. This part is more challenging because it is difficult in some part of the scapula to decide based on the grey values if it is either cortical or trabecular bone.

---

<sup>2</sup>Dassault Systèmes, France.



(a) Common cortical contour for both segmentation methods  
 (b) Superimposition of the two trabecular obtained. Pink is for the manual and yellow is for the semi-automated segmentation

Figure 2.2: Different bone volume obtained after the segmentation process

This can be due to inhomogeneous bone structure, low contrast edges due to osteoporosis, partial volume effect, etc.

As it can be observed in the figures 2.2b 2.3 and 2.4, a difference between the trabecular bone segmented using the manual and the semi-automated segmentation method is present. In some region this difference is quite important. One can easily hypothesise that the segmentation process will have an effect on the modelling outputs.

All the segmentation process were realised with big care because the quality of the final model is dependent on the quality of the segmentation and moreover, as the aim of this work was to investigated if the two segmentation methods induce differences in the simulation outputs, one want to add as less as possible external errors.

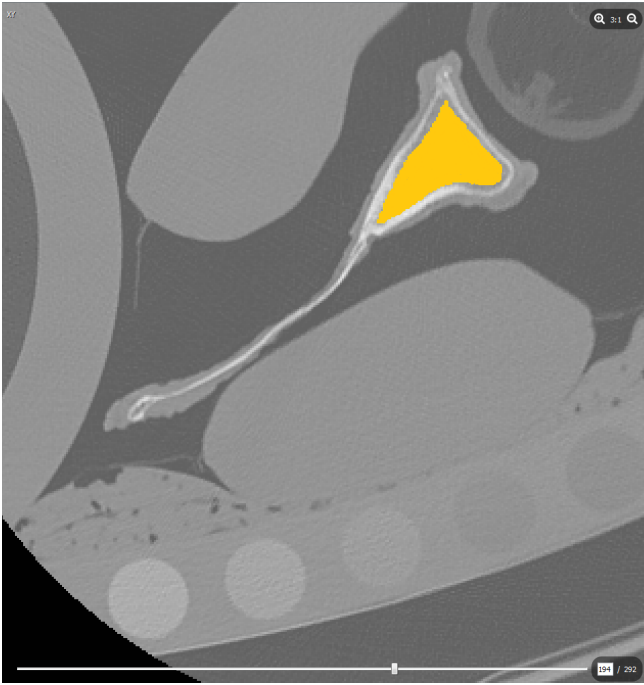
## 2.3 Smoothing

The obtained segmented geometries were smoothed in Amira and then exported. They were then imported in Geomagic<sup>3</sup> to repair eventual holes, which occur when some segmented surfaces were too fine. They were also smoothed and other geometry problems were repaired. The scapula was then cut at its backside. Indeed, it was shown<sup>4</sup> that after a certain distance perpendicular to the glenoid cavity, the applied force (in the FE simulation) was not influencing the stress and strain

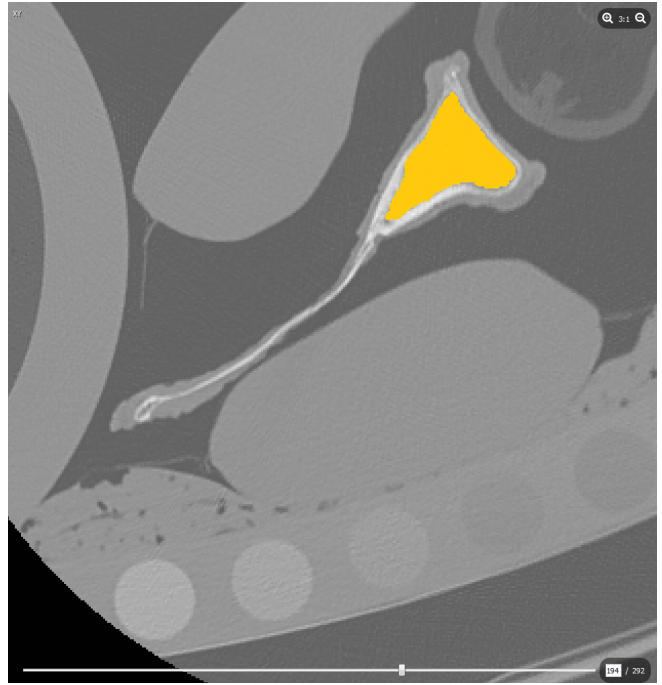
<sup>3</sup>3D Systems, North Carolina, USA.

<sup>4</sup>Internal study of the LBO.



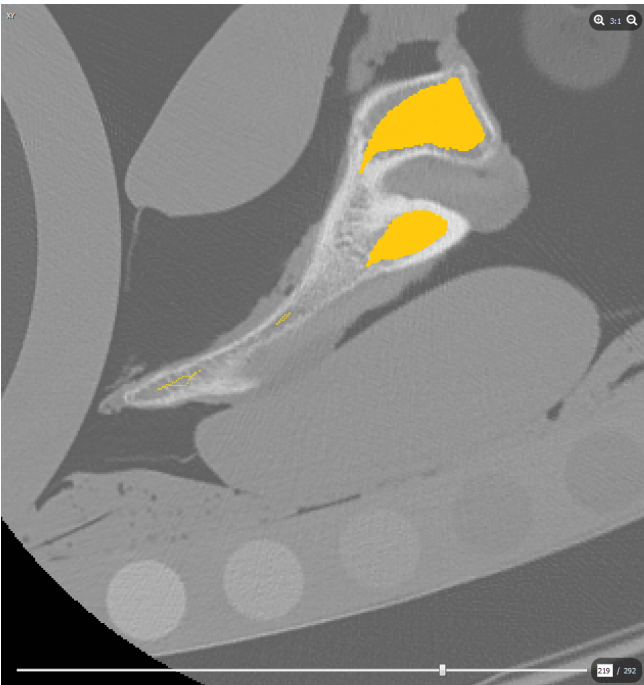


(a) Semi-automated segmentation

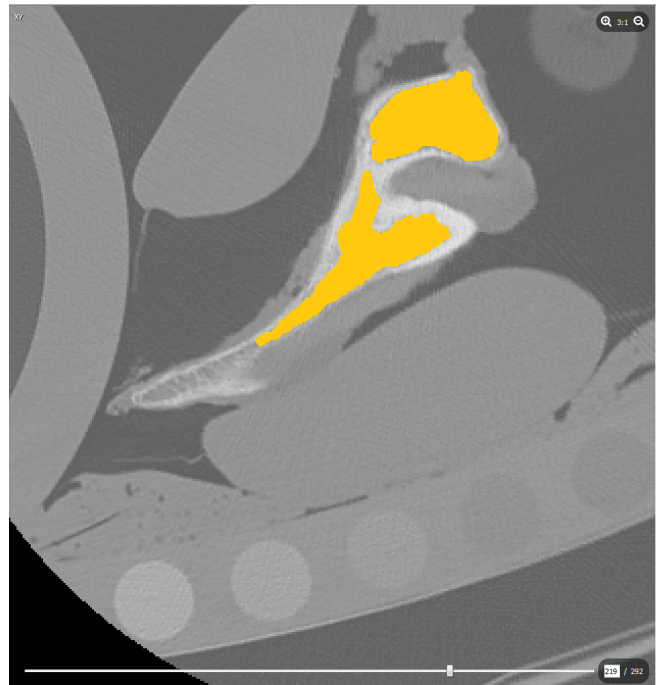


(b) Manual segmentation

Figure 2.3: Differences between the two segmentation method for the trabecular bone (yellow). The same slice on the CT data is selected.



(a) Semi-automated segmentation



(b) Manual segmentation

Figure 2.4: Differences between the two segmentation method for the trabecular bone (yellow). The same slice on the CT data is selected.

anymore in the glenoid cavity. So the scapula geometry was cut by a plane, in parallel with the sagittal plane, after the scapula notch. The three segmented geometries obtained following the two different segmentation methods were cut by exactly the same plane.

## 2.4 Cortical geometry

As the three parts (trabecular "manual", trabecular "automatic", cortical "contour") were cut in Geomagic, they were imported in Solidworks, where they were closed and filled.

In order to have the real cortical geometry, the cortical contour and the trabecular geometry were imported together in Solidworks and substracted. Indeed, as they were cut by exactly the same plane, the cortical contour and the trabecular part were placed and constraint by the cutting plane of each part, to ensure that they were correctly placed one with respect to the other. The two parts were then substracted and the cortical geometry was then obtained. This procedure was realised for the both methods, the automatic and the manual one. It is important to emphasise that the cortical contour is the same for the automatic and the manual method.

## 2.5 Virtual arthroplasty

To realise the virtual arthroplasty, an assembly of the scapula with the prosthesis was made in Solidworks. The cortical and the trabecular bone parts were imported in the assembly and constrained together by their medial backside surface. The implant, the cement, and the cutting tool were imported in the same assembly.

### 2.5.1 Implant selection and placement

The selection of the implant and its placement in the scapula are made by the surgeon, and follow the manufacturer recommendations. As the implantation of the studied cadaveric scapula was not already planned, the choice of the prosthesis and its placement were made based on basic preoperative instructions. The selected glenoid implant was an Aequalis PerForm (M35 Keeled Glenoid, Ref: DWE512) furnished by Tornier<sup>5</sup>. The size was chosen to fit as well as possible the glenoid cavity and the implant was placed in order to preserve as much as possible cortical bone<sup>6</sup>.

With the implant geometry, the geometry of a tool "Outil Perform" was also provided. In fact, during the surgery, before to place and cement the implant in the scapula, the glenoid surface has to be prepared and holed. This is done by the use of different specific tools. The "Outil Perform" provided, simulated the action of those specific tools. In the software, to realise the virtual arthroplasty, the "Outil Perform" was constrained with the implant, and when the implant was correctly placed, the trabecular and cortical parts were cut by this tool. Then as the implant was positioned in the scapula, all the parts except the cutting tool were exported in step format.

---

<sup>5</sup>TORNIER, Group Wright, Montbonnot, France.

<sup>6</sup>TORNIER, Group Wright, Aequalis Perform, Glenoid system, Surgical technique, 36 p.

## 2.6 Finite element model

In order to compare the two different segmentation methods used, a finite element model was built. The FE model was realised with the software Abaqus<sup>7</sup>. A linear static analysis was realised on both cases with the given conditions which will be detailed later. For each part a CAO geometry in STEP format was imported.

### 2.6.1 Geometry

The whole system was composed of four elements, the scapula, the implant, the cement and the humeral head.

Although the cortical and trabecular bone were segmented, smoothed and placed distinctly, they just formed one bone part in the FEM. Indeed, to better model the interactions at the cortical/-trabecular interface, the two parts were correctly placed and constrained in Solidworks, and then exported as one part for the simulation in Abaqus. The different bone parts were still distinguishable for the material assignment.

The different parts constituting the prosthesis (implant and cement) did not undergo any change from Solidworks to Abaqus.

In order to be closer to the reality, and as only the geometry of the scapula itself was available, the humerus was created in Abaqus. It was modelled as a hollow semi-sphere with 43 mm radius and was considered as a rigid body in the simulation. Indeed, in implemented patients, the humeral head is replaced by an implant made of a CoCr alloy, whose elastic modulus (E) is 220 GPa. So the humeral head can be taken as a rigid body with respect to the implant, whose elastic modulus is 720 MPa. The dimension chosen was based on average patients' data available.

For this study, a 3D simulation was realised.

### 2.6.2 Material properties

All the materials used were considered linear, elastic, homogeneous and isotropic. These hypothesis were made in order to simplify the reality and thus the simulation but the materials and especially the cortical and trabecular bone are not homogeneous and isotropic in reality. The assigned properties were based on a previous study[15] and manufacturer data.

Below is a table resuming the constituent properties of the materials [10] [11].

Sections in 3D were used. They are homogeneous and isotropic for each material. Although the scapula was represented in one part, it had two different section assignments. The scapula was divided in two regions, the cortical and the trabecular bone. Each region was assigned to its corresponding section.

### 2.6.3 Surface interactions

An assembly with all the parts was made and thus interactions between the different parts were defined. The modelling of these interactions was realised through the use of "Bilateral constraints",

---

<sup>7</sup>Dassault Systems, Vélizy-Villacoublay, Île-de-France, France

Material	Elastic modulus E [MPa]	Poisson's ratio $\nu$ [-]	Yield stress [MPa] *fatigue	Ultimate stress [MPa]
Cortical bone	11500	0.3	120	133 (Comp.)
Trabecular bone	500	0.3	1.92	5.33
Implant (UHMWPE)	720	0.4	19 (Tens.) 18*	27 (Tens.)
Cement (PMMA)	2000	0.23	7*	25 (Tens.) 80 (Comp.)

Table 2.1: Materials properties

which allow to fix the separated parts together. More in details, "Surface to surface" interactions were used. Three interactions were defined: Bone-Cement, Cement-Implant, Implant-Humeral sphere. For the Bone-Cement and Cement-Implant interactions, a "Tie" constraint was used. It allows to link the two parts and to ensure continuity of the displacements. Indeed, a master and a slave surface are defined and are then linked together through kinematic equations to keep the relative position constant between each point of the slave surface and its corresponding projection on the master surface. For the Implant-Humeral sphere interaction, a contact with friction-less tangential behaviour is imposed.

#### 2.6.4 Loading hypothesis

To define the boundary conditions and the applied load, two coordinate systems were used, the global of Abaqus and an another one was created. The "user-defined" coordinate system was used to apply the load and the boundary conditions of the humeral head. It was a cartesian coordinate system with origin in the centre of the humeral head, y-direction in the medial direction, and x-direction in the anterior direction. All the boundary conditions and applied load were spatially defined and not temporally.

##### **Boundary conditions:**

The scapula was fixed at its proximal side. The surface resulting from the previous cut of the scapula was selected and fixed in displacement in the three space directions ( $U_1=U_2=U_3=0$ ). This was done in the global coordinate system.

The humeral head was allowed to translate spatially, but was not allowed to rotate. Indeed, the humeral head penetrate and deform the implant. Thus it was fixed in the three degrees of rotation ( $UR_1=UR_2=UR_3=0$ ). These conditions were defined in the "user-defined" coordinate system.

##### **Load:**

In this study, one load case was considered. A concentrated static axial force of 750 N was applied on the humeral head along the medial direction. It was defined in the "user-defined" coordinate system along the y-direction. The force value and its direction where taken from the ASTM Norm for "Strandard Test Methods for Dynamic Evaluation of Glenoid Loosening or Dissociation"[13].

### 2.6.5 Mesh

Elements of type "Tetrahedric-Free" (C3D10) were used because they allow to mesh all the different parts. Quadratic form functions were taken because it speeds up the convergence of the simulation, and exact integration was used. Each part was differently globally seeded. As the trabecular and the cortical bone form one part, they are meshed together with a global seed size of 3 mm. The cement was meshed with a global seed size of 0.8 mm and the implant with 1.15 mm. The humeral head was not meshed because it is considered as a rigid body.

None convergence analysis was realised because the mesh hypothesis were taken from another study[14], whose purpose was the convergence analysis. Indeed, the same outputs as in this study were investigated.

### 2.6.6 Outputs

In order to analyse the results and realise the statistical analysis, the stress and strain values were considered for the scapula and the cement part. More precisely, for the scapula, von Mises stress and octahedral shear strain were taken as outputs and are defined like:

- Von Mises stress:  $\sigma_e = \frac{1}{\sqrt{2}} \sqrt{(\sigma_1 - \sigma_2)^2 + (\sigma_2 - \sigma_3)^2 + (\sigma_3 - \sigma_1)^2}$
- Octahedral shear strain:  $\gamma_{oct} = \frac{2}{3} \sqrt{(\epsilon_{11} - \epsilon_{22})^2 + (\epsilon_{11} - \epsilon_{33})^2 + (\epsilon_{22} - \epsilon_{33})^2 + 6(\epsilon_{12}^2 + \epsilon_{13}^2 + \epsilon_{23}^2)}$

For the cement part, octahedral shear strain and minimum principal stress were investigated. Indeed, as the cement was loaded in axial compression, it was more relevant to consider the minimum principal stress instead of the von Mises stress. Moreover, such outputs were taken because they are commonly used in the literature[1] [2] [7] and allow to be consistent with other studies in progress in the laboratory.

The volume at each integration point (IVOL) was also extracted and allowed to compute stress and strain distributions in the scapula. As tetrahedric elements were used for the mesh, each element has four integration points, so the stress and strain values were extracted at these four points for each elements.

## 2.7 Statistical analysis

In order to estimate the error if there is one, between the semi-automated and the manual segmentation, comparison of the results for the both methods and the guidelines for a statistical analysis are given. First, an overview of what is usually done to compare methods or extract statistical significance in the biomechanical field, is made. Then the different steps needed to realise it are explained in more details.

### 2.7.1 Methods overview

**Outputs:** First of all, to compare or extract statistical significance from data, one should know which data to extract and compare. This will also define the output require from the FE simulation. In a publication of A. Terrier et al. [2], they investigated if there was a correlation between the

cement stress predictions after a total shoulder arthroplasty and the preoperative glenoid bone quality. To do so, from the FE model, they extracted the cement stress, the bone-cement interfacial stress, the bone strain and the VOI volumes. In another publication, Andrew E. Anderson et al. [7], developed a subject-specific FE model of the pelvis and realised a sensitivity study. They compared experimental measurements and FE measurements. From the FE model, they took out the von Mises stresses and the principal strains values of the bone. An other group [8], tried to estimate the uncertainties on the accuracy of patient-specific FE models of the scapula. They studied the uncertainties of different steps involved in the creation of the FE model, whose were, the bone density, the musculoskeletal loads and the material mapping relationship. This group investigated if those uncertainties had an impact on the predicted strain distributions. To do so, they took out the maximum and minimum principal strains of the FE simulation.

**Methods comparison:** Once the FE model outputs are obtained, one need to compare them if two different methods are used to quantify the same quantity. To compare results of different methods, G. Campoli et al. [8], built a reference scapula model, and quantify the deviation of the other models with respect to the reference one.

### **Statistical analysis:**

To realise a statistical analysis, ones needs many scapulae to be able to test correlations. In this work, only one cadaveric scapula is segmented, so no statistical analysis could be perform, but as this project is part of a bigger study where twenty cadaveric scapulae are available, the statistical analysis guidelines are given.

First, a little summary of the tools used in the publications cited above is made.

A. Terrier et al. [2] calculated the linear correlations between patient characteristic CT measurements and FE predictions. The correlation strength was evaluated with the Pearson correlation coefficient ( $r$ ) and its associated P value. The statistical significance was set to  $P < .05$ . Andrew A. Anderson et al.[7] also calculated the best-fit lines and  $r^2$  values and set the statistical significance to  $P < .05$ .

Moreover, as different scapulae and observers were involved in the study of A. Terrier et al.[1] and Jacob F. Kidder et al.[9], the inter- and intra- observer reproducibility was assessed. This was measured with the correlation coefficients (ICCs). Indeed, some process involved in the FE model and some calculations could differ because they involved the observer self decision or knowledge. So it is important to assess the conformity among observers. For example, the manual segmentation step is only based on the observer self assignment of each pixel to one class. So in order to test the error between the observers, the inter-observer reproducibility is assessed (agreement). One should also check the intra-observer reproducibility. The intra-observer assesses the reproducibility of the measurements made by one observer measuring the same quantity but after a certain time and shows if one observer has always a particular deviation (consistency). There exist different tables that rate the inter/intra-observers reproducibility, but in any case, the more the ICCs coefficients are close to 1, the more the reproducibility of the results is high.

To asses the inter/intra-observer reproducibility, A. Terrier et al.[2] had two evaluators who evaluated (segmented) 107 CT scans of scapulae and the evaluation was checked by a radiologist. After two weeks, twenty scapulae were re-measured. In the study of Jacob F. Kidder et al.[9], three evaluators were involved in the evaluation process, and did re-measurements after one week

interval in a random order.

### 2.7.2 Application to this work

As mentioned earlier, in this work only one cadaveric scapula was segmented. So no statistical analysis could be performed. Indeed, it is difficult to establish correlations with just one input/output. This also leads for the inter/intra-observer reproducibility.

But as many (twenty) cadaveric scapulae CT scans are available, it could be interesting to apply the workflow on all of them. Because one does not know if the conclusions that will be given in this work are the same for all the scapulae, and moreover, as the segmentation process and especially the manual segmentation is the step where most of errors with respect to the reality can be integrated, one should check the inter/intra-observer reproducibility.

On the other hand, has two different segmentation methods are tested, two different sets of outputs will be available, so a comparison between them can be perform. In conclusion, to estimate the errors between the semi-automated and the manual segmentation, a comparison between the stress and strain values in the scapula (and in the cement) will be carry out. No reference model is available in contrary to the study of G. Campoli et al.[8], so the deviation will be define as the deviation between the two models and not with the reference one.

## 3 Results

In this section, the different results obtained are presented. Unfortunately, the simulation of the manually segmented scapula did not succeed and thus no outputs were available from the FE simulation. Thus no comparison could be done. Only the results of the semi-automated scapula are given. The stress and strain values were extracted and computed by a user-defined Python and a Matlab<sup>8</sup> script.

### 3.1 Bone

In the figures 3.1 and 3.2 the relative cumulative volume of von Mises stress and octahedral shear strain are plotted for the bone (cortical and trabecular). In the figure 3.1, one remarks that 70% of the bone is subjected to 1 MPa of von Mises stress. Less than 5% undergo 2 MPa. The maximum von Mises stress was 75.11 MPa. This value was only achieved for one mesh node of the bone. This maximum was located in the anterior-frontal plane, just behind the glenoid cavity in the cortical bone. Otherwise, the main stresses were located in the glenoid cavity on the anterior side of the hole (where the implant keel is placed). The stress was also higher in the 3mm cortical layer in contact with the cement. The von Mises stress was mainly located in the cortical bone. The trabecular bone underwent some stress but its highest value was 19.99 MPa and was reached for the elements at the interface between the two types of bone in the keel hole.

---

<sup>8</sup>The MathWorks, Natick, MA, USA

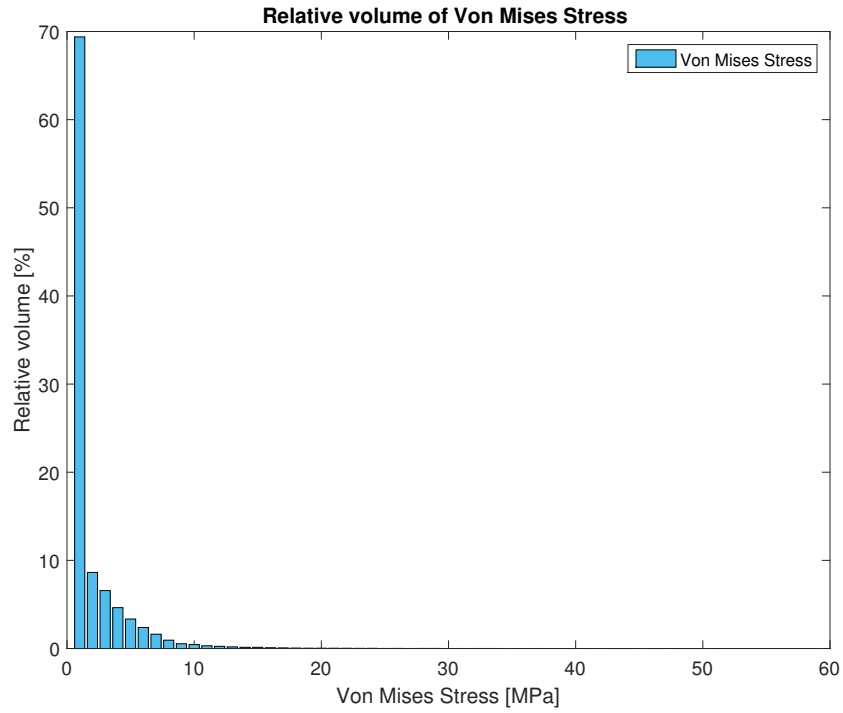


Figure 3.1: Relative volume of the bone which undergo Von Mises stress (MPa).

For the octahedral shear strain, 60% of the scapula undergoes 0.001 MPa and the maximum octahedral shear strain value is 0.025 MPa. Moreover, the maximum principal strain was achieved in the trabecular bone and its value was 0.03 MPa. This maximum took place in the trabecular bone at the interface between the cortical and the trabecular bone. It was located on the upper anterior edge of the hole in the scapula (where the implant keel is placed). Almost none strain was recorded in the cortical bone.



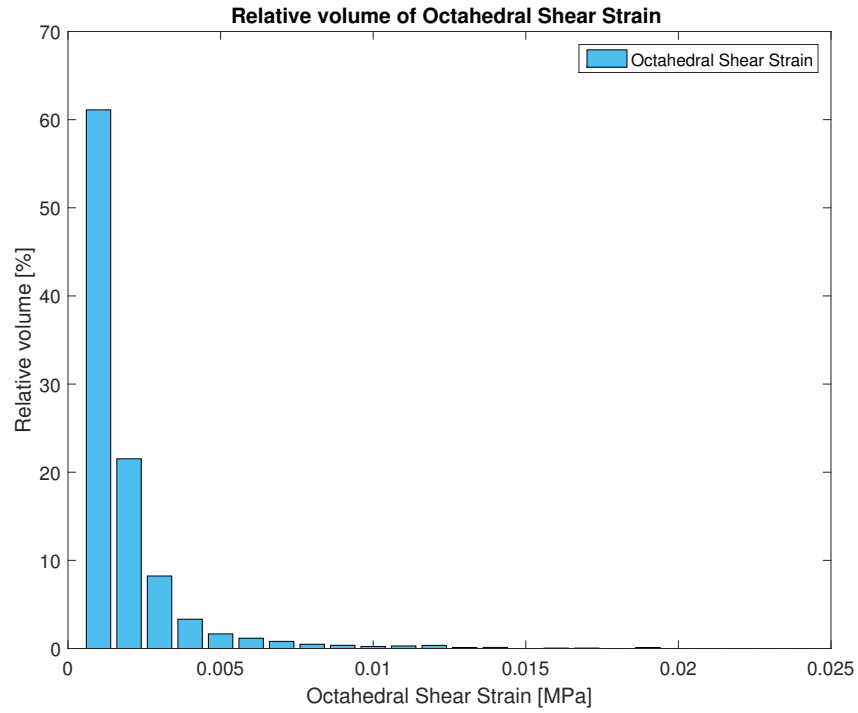


Figure 3.2: Relative volume of the bone which undergo octahedral shear strain.

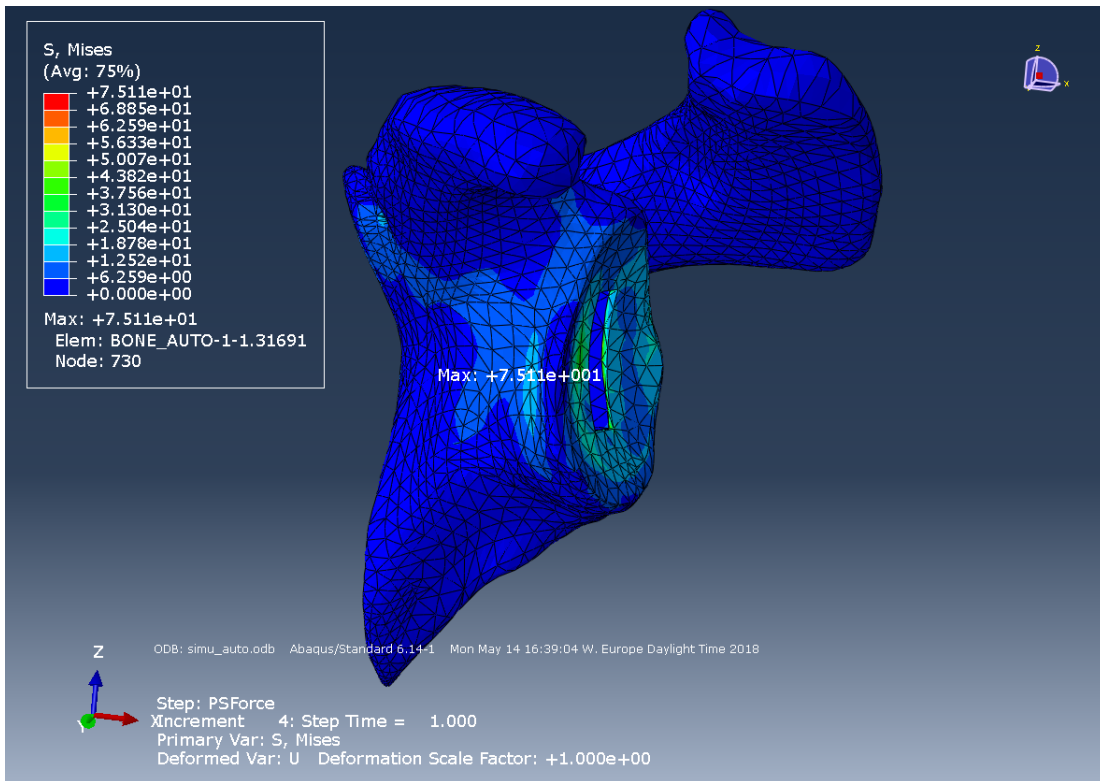


Figure 3.3: Contour of the von Mises stress on the semi-automated segmented scapula

## 3.2 Cement

The stresses and strains values for the cement are more distributed than those of the bone, and higher.

Looking at the figure 3.4, 40% of the cement part undergoes 2 MPa and 25% undergoes 1 MPa. The highest minimum principal stress was 13.6 MPa and located on the keel part on the face in contact with the bone, and 0.8-1.6 mm away from its backside.

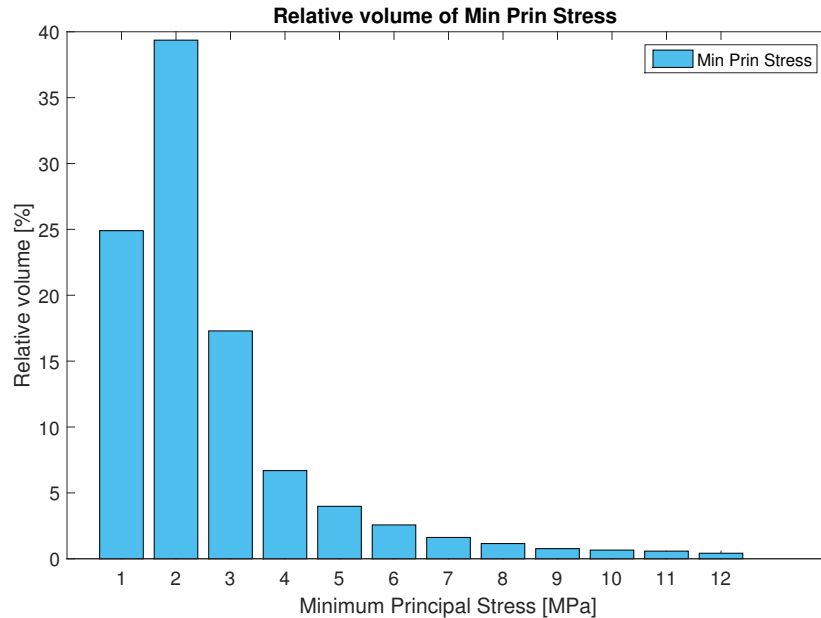


Figure 3.4: Relative volume of the cement which undergo minimum principal stress.

For the octahedral shear strain, more than 25% of the cement undergo 0.003 MPa and 20% undergo 0.002 MPa. The maximum computed octahedral shear strain was 0.035 MPa. Moreover, the maximum principal strain was 0.05 MPa and was located on the keel surface in contact with the bone on the posterior-frontal side. Otherwise, the main strain areas were located all around the keel surface which is in contact with the bone, at 0.8-1.6mm from the cement backside.

## 4 Discussion

### 4.1 Semi-automated segmentation

#### 4.1.1 Bone

The main von Mises stress in the scapula was equal to 1 MPa and was thus not exceeding the yield stress (Table 2.1). The few elements that exhibited more than the yield stress fatigue value were all located in the glenoid cavity, in the cortical in the hole where the implant was placed, and at the base of the acromion. None of them were exceeding the ultimate stress value. So no fracture of the bone should occur, but deformations in case of constant repeating loading can occur in the glenoid cavity. The von Mises stress was much higher for the cortical bone than for the trabecular one. It was expected that the main stress was located in the glenoid cavity, and in the hole made

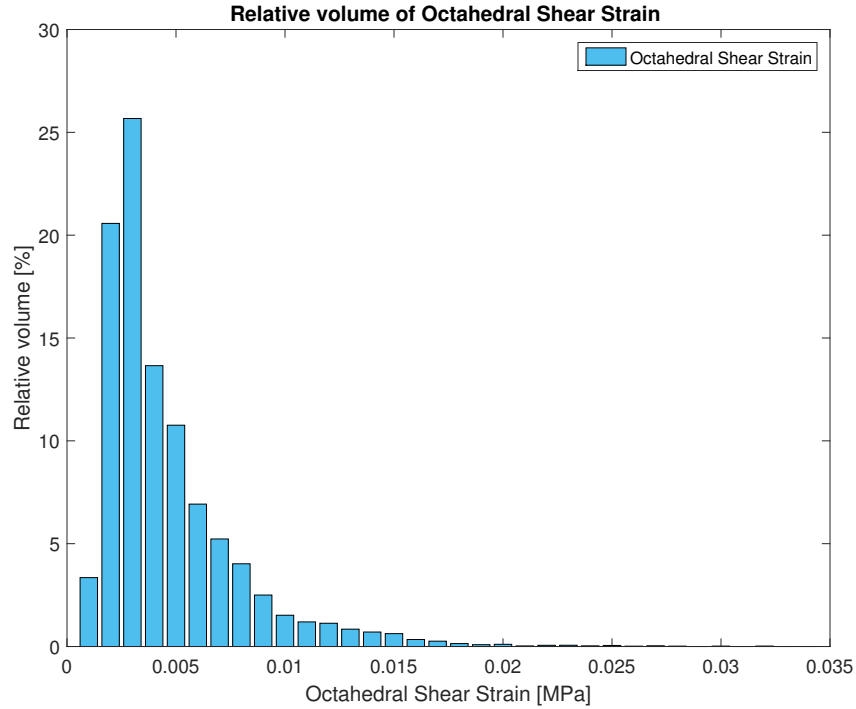


Figure 3.5: Relative volume of the cement which undergo octahedral shear strain.

by the implant, as the applied load is transfer to the scapula by the contact between the cement and the bone. So all the faces in contact with the cement underwent the main stress. Moreover, the stress is highly located in the cortical part, which is good in term of bone damaging. Indeed, the cortical bone has a higher elastic modulus and can support higher stress than the trabecular bone. The most loaded part in the trabecular bone is the subchondral trabecular bone (ST) which is in contact with the cortical layer of the glenoid cavity. These results seem coherent, as the glenoid cavity is the most loaded region of the scapula.

The strain was mostly present in the trabecular bone which is in contact with the cortical layer in the glenoid cavity. The maximum values did not exceed the critical ones, expect for a few elements of the trabecular bone in contact with the cement and located at the interface between the two types of bone. So micro cracks could appear at this place but very locally.

#### 4.1.2 Cement

The maximum value of minimum principal stress was equal to 13.16 MPa, which is higher than the fatigue yield stress of the cement. But only very few elements were exceeded this fatigue yield stress. They were all located on the keel outside surface near to the backside. So the cement will begin to plastify a bit a those places, but it is acceptable, and it was expected. Indeed, studies reported that stress in the cement is mainly located in the keel and backside region[2].

The maximum strain in the cement was located at the same places as the stress. Indeed, it is higher in the keel hole, in the backside, and principally on the keel outer surface in contact with the bone and close to the backside.

In general, the stress and strain values were on average higher in the cement than in the bone. They were also more distributed in term of relative volume. So the cement is the most critical part of the assembly in this case.

It should be noticed that the loading case was not representing the exact loading reality, but a simple case taken from ASTM Norm, as the aim of the work is not to have a model very close to the patient loading, but to estimate variations between two methods. In fact, in the future, cadaveric scapulae are going to be loaded the same way in an experimental set-up. Indeed, a further step will be to validate the FE model with the experiment, so the same load case has to be applied. Moreover, the above discussion about the stress and strain values shows that the built model is correct with respect to what is normally found in the literature. So it could be use to perform the error estimation as its outputs are not out of sense.

## 4.2 Manual segmentation

Unfortunately, the generation of the finite element model caused much problems for the manually segmented bone part and thus this step could not be completed and no outputs were available to realise the error estimation. Indeed, as the geometry was imported in the FE software, it suffered from lots of invalid geometries and the software was not able to generate a proper mesh of this part. This may be due to the fact that the cortical layer is extremely fine at some places in the bone, especially in the glenoid cavity, which is the main region of interest. In order to deal with this problem, the different steps involved in the patient-specific model workflow were investigated. First, the geometry underwent geometry repair processes, but this was not sufficient. Then small seeding mesh of the size of the small cortical layer were applied, but anyway, this did not resolve the problem. In the figure 4.1 the highlighted elements are ones who cause problem. If those elements were only located in the acromion or in the coracoid process, the geometry could have been cut at this place and the results would not have been influenced. But some of them are located in the glenoid cavity.

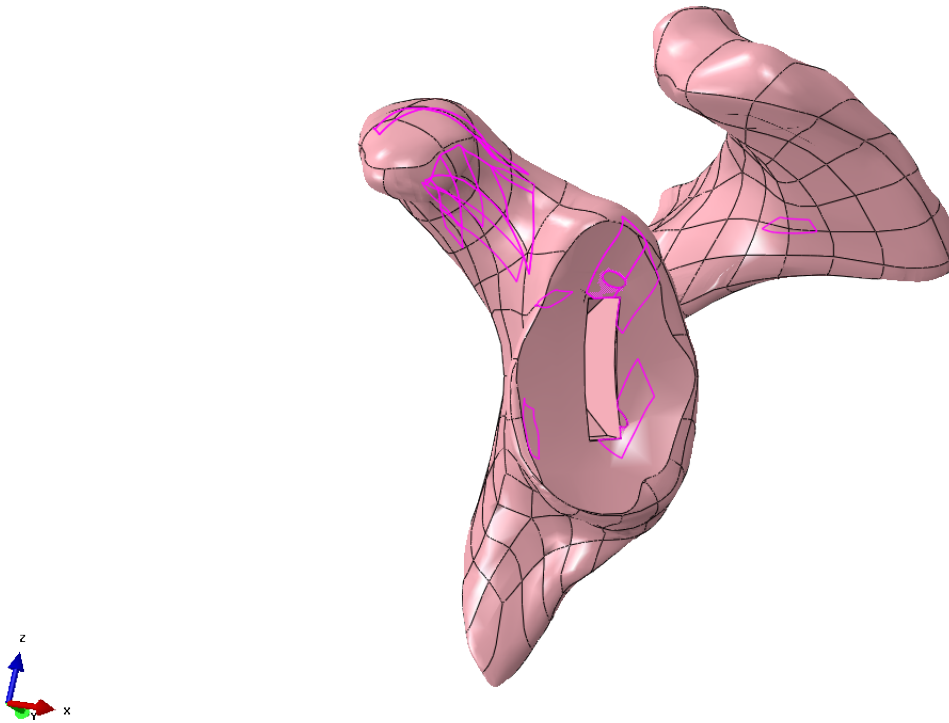


Figure 4.1: Manually segmented scapula, where highlighted regions are the ones that the program could not deal with.

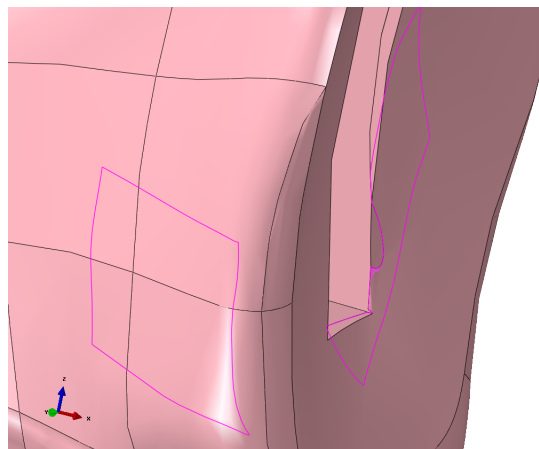


Figure 4.2: Zoom on the glenoid cavity of the manually segmented scapula, where highlighted regions are the ones that the program could not deal with.

At some points in the glenoid cavity, the trabecular bone was directly exposed and thus in contact with the cement part as it can be seen in the figure 4.2. As normally during the surgery, the surgeon tries to not cut the cortical layer at this place and preserve it as much as possible, the

virtual arthroplasty step was performed again. There, the implant was positioned again, but less deeper into the scapula in order to preserve all the cortical layer which was segmented. This did not fix the problem. Indeed, the cortical layer is inherently extremely fine in this region of the scapula, as it can be observed in the figure 4.3.

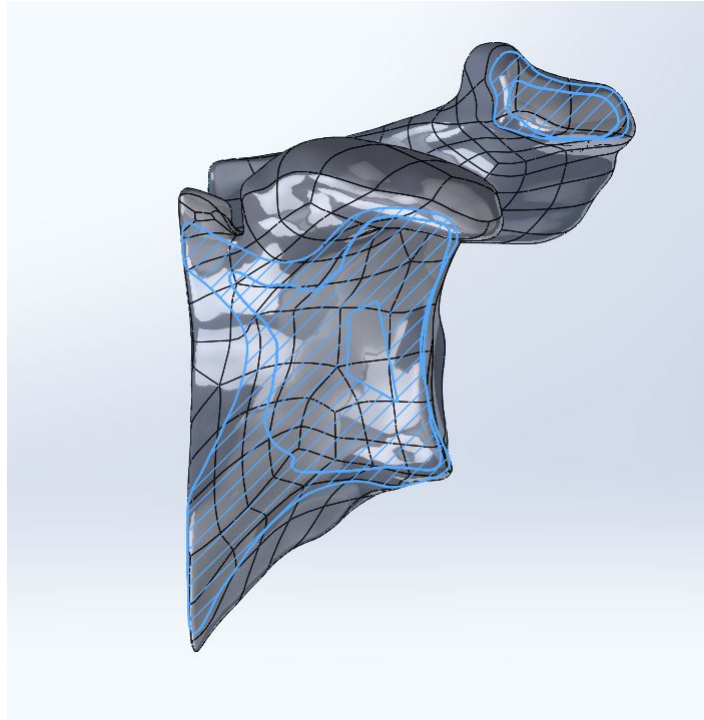


Figure 4.3: Cut of the manually segmented scapula parallel to the frontal plane. The delimited closed regions are the cortical and trabecular boundaries.

The last step to "retouch" was the segmentation step. But this could not be done because otherwise, influences would have been introduced, which would have falsify the study of the errors between the two segmentation methods. Indeed, as the identified problem was the finesse of the cortical layer, someone could have thought to thicken it. But then, the manual segmentation obtained would not be the right one.

## 5 Limitations and further improvements

The error estimation which was the goal of this project, could be improved by different ways, and the accuracy of the conclusion also. Moreover, different steps involve in the workflow used to build the "cadaver"-specific model can also be improved. Indeed, the "cadaver"-specific model was built with simple hypothesis through the different steps, and improvements of such steps are available and need to be implemented on this model, in order to be more "cadaver"-specific.

### 5.1 Manual segmentation workflow

As the main problem of the manual segmentation was that the FE software could not deal with the highly number of geometry invalidities especially in the the glenoid cavity, and thus was not

able to generate a proper mesh, one solution could be to use a more sophisticated algorithm for the mesh generation. Indeed, different meshing methods such as "Structure-based" meshing[6] which uses geometrical information of the whole bone to generate a more advanced mesh can be applied.

The invalid geometries were due to the extreme thin cortical thickness. The segmented scapula owned to an old donor, and this thin cortical thickness could be due to the age of the donor. An other cause could be that as the manual segmentation process represents more accurately the bone structure and thus is more geometry dependent. So maybe the geometry of the considered scapula is not adapted to this method. In conclusion, a solution could be to perform the error estimation on an other scapula which has inherently an higher cortical thickness.

## 5.2 Statistical analysis

As one scapula was segmented in this project, no statistical analysis could have been conducted. But in the future, as twenty CT data of cadaveric scapulae are available and accessible by the laboratory, the differences between the two methods of segmentation treated in this work, could be assessed on each of those scapulae. Indeed, the conclusion of this work just take into account the results of one segmented scapula. But one needs to prove that such conclusions can be extended to other cases in order to draw a general conclusion.

Then, if multiple scapulae segmented by these two methods are available, correlations between scapula characteristic measurements and FE outputs can be investigate. And the method described in the "Methods" section can be applied.

When a statistical analysis is performed, one also needs to check the inter/intra-observer reproducibility. Indeed, one observer could induce a constant variance on the results, or if different observers treat the data, there could be errors between them.

## 5.3 Manual segmentation control

As already said, the segmentation process is the more consuming step of the workflow to create a patient-specific model. And this process is dependent of the observer knowledge and estimate. Moreover, to have a good quality on the results and the conclusions given, the quality of the segmentation needs to be good. This is especially the case for the manual segmentation because nothing is automated in this method, and thus it is more subject to induced observer errors. As Poelert et al. [6] wrote: "The quality of the final model is very much dependent on the quality of the segmentation...."<sup>9</sup> and the: "Uncertainty in the segmentation can translate into a much larger uncertainty of the modelling output."<sup>10</sup>. To overcome this uncertainty in the segmentation or reduce it, the segmented bone can be shown to a musculoskeletal radiologist or a surgeon. This is often used in the research [1].

---

<sup>9</sup>Poelert, p.467

<sup>10</sup>Poelert, p.468

## 5.4 Material inhomogeneity

All the materials used to build the FE model were considered homogeneous. This assumption is highly questionable for the bone part. There exists a Matlab<sup>11</sup> script in the laboratory (LBO), which derived the elastic modulus at each node of the bone part by the use of a material mapping relationship. This script extracts the local bone density at each node, which is derived from the (HU) values of the CT data. This script can not be run on this case, because it needs reference points on the scapula, whose are computed by an other Matlab script. And this other script can also not be run on this case, because it needs to have the humeral head position, which is not available with the CT data provided of the cadaveric scapula. So as an improvement step, one could adapt the existing scripts that work for patients CT data, to cadaveric scapulae.

This improvement should influence the elastic modulus, because it has been shown that this one is affected by the bone density.

## 5.5 Material anisotropy

The materials considered in this work were all considered isotropic. This can be false, especially for the trabecular bone. Indeed, the trabecular bone is composed of lots of trabeculae whose are not isotropically dispersed in space and thus create anisotropy. When one assume that the trabecular bone is isotropic, its stiffness is derived from the (HU) values of the CT scan and computed using bone density-elasticity correlation. Thus, the complex microstructures of this type of bone is approximated by macrostructural continuous constitutive relationship. But it is known that trabecular has a preferable growth direction, and this means that its mechanical behaviour is anisotropic. Furthermore, it was reported that this anisotropy increases when the bone suffers from osteoporotic state [6].

One way of taking this anisotropy into account, is the use of micro-FE model. Such models could be build for the cadaveric scapulae, because micro-CT data are available. Indeed, the scapula in contrary to a whole patient body, is small enough to enter a micro-CT scanner. But still now, researchers are not agree on the benefits, that the modelling of the trabecular anisotropy could have. Moreover, the modelling of this macroscale behaviour is more computationally demanding [6].

## 5.6 Prosthesis choice and placement

For the sake to be more patient-specific, the prosthesis choice and placement should be approved by a surgeon although it was still placed based on basic preoperative instructions. This normally should not change the conclusions on the comparison of the two segmentation methods, but will certainly change a bit the values of stress and strain obtained.

---

<sup>11</sup>MathWorks, Natick, Massachusetts, USA.



## 6 Conclusion

The goal of this project was to estimate the errors between two segmentation methods. Indeed, despite the fact that the segmentation process is largely used to extract bone geometry and thus build patient-specific models, its uncertainty has not been assessed. Moreover, it is commonly admitted by the scientific community that uncertainty in the segmentation process, can leads to a larger uncertainty on the finite element model outputs. But this was never scientifically and rigorously proved.

In order to begin answering this question, two segmentation methods were firstly investigated. They were both applied on the same cadaveric scapula. The considered methods were the manual and semi-automated segmentation. The manual segmentation was performed by the use of thresholds values and manual adjustments. The semi-automated segmentation, is more automatised than the first method. Indeed, in contrary to the manual segmentation, in the semi-automated segmentation, only the cortical bone was generated by manual segmentation. The trabecular bone was obtained by a shrunk of the manually segmented cortical contour. Then a cortical layer of three millimetres thickness was obtained for the cortical bone of the semi-automated method. This thickness is the same used by A. Terrier et al.[2], which derived this cortical thickness by the analyse of CT images and previous reported values for subchondral bone thickness. To estimate the error between the two methods, a comparison of the outputs of the two FE models was proposed.

The modelling outputs of the FE model based on the semi-automated segmentation were coherent to what was expected and to what is normally found in the literature. The aim of the work was not to reproduced exactly the patient-specific loading case, placement, or material mapping as these considerations should not influence the comparison of the two methods. But the results allowed to know that the simplified FE model built was at least good, and suffered from no implementation errors. Unfortunately, no outputs of the FE model based on the manual segmentation were available. Indeed, due to the extremely thin cortical thickness in the glenoid cavity, the model contained invalid geometries and the FE software was not able to mesh the bone part. Different steps of the workflow were investigated in details in order to deal with this problem. One of the main try was to reposition the implant to maintain as much as possible cortical bone in the glenoid cavity. But as the cortical was inherently thin in the segmented scapula, this did not solve the problem. The only way to deal with it, would have be to thicken the cortical layer in this region in the segmentation process. But this will then have induced influences and errors in the conclusion of this work.

A way to achieved the comparison between the methods, would be to use a more sophisticated meshing algorithm able to deal with complex geometries. An other way could be to realise the study on an other scapula which cortical thickness is inherently thicker.

In comparison to the manual segmentation, the semi-automated method offers lots of advantages. Indeed, as it has been experienced in this work, the workflow is less challenging, this method is less time consuming and less variance across observers happier. So this method appeared to be promising in a sense that it could be included in a routine preoperative planning or in a CT scanner directly. Effectively, at this moment, fully automated segmentation methods based on machine learning algorithms are developed. Thus knowing the error made at this step is primary.

## References

- [1] Terrier A, Ston J, Dewarrat A, Becce F, Farron A. A semi-automated quantitative CT method for measuring rotator cuff muscle degeneration in shoulders with primary osteoarthritis. *Orthopaedics & Traumatology: Surgery & Research*. 2017;103:151-157.
- [2] Terrier A, Obrist R, Becce F, Farron A. Cement stress predictions after anatomic total shoulder arthroplasty are correlated with preoperative glenoid bone quality. *J Shoulder Elbow Surg*. 2017;26:1644-1652.
- [3] AlZu'bi S, Amira A. 3D Medical volume segmentation using hybrid multiresolution statistical approaches. *Advances in Artificial Intelligence*. 2010;520427:15 p.
- [4] Montgomery D, Amira A, zaidi H. Fully automated segmentation of oncological PET volumes using a combined multiscale and statistical model. *Am. Assoc. Phys. Med.*. 2007;34(2): 722-736.
- [5] Hoenecke Jr. Heinz R, Hermida Juan C, Flores-Hernandez C, D'Lima Darryl D. Accuracy of CT-based measurements of glenoid version for total shoulder arthroplasty. *J Shoulder Elbow Surg*. 2010;19:166-171.
- [6] Poelert S, Valstar E, Weinans H, Zadpoor A. Patient-specific finite element modelling of bones. *J Engineering in Medicine*. 2012;227(4): 464-478.
- [7] Anderson AE, Peters CL, Tuttle BD, Weiss JA. Subject-specific finite element model of the pelvis: development, validation and sensitivity studies. *J Biomech Eng* 2005;127(3): 364-373.
- [8] Campoli G, Bolsterlee B, van der Helm F, Weinans H, Zadpoor AA. Effects of densitometry, material mapping and load estimation uncertainties on the accuracy of patient-specific finite-element models of the scapula. *J. R. Soc. Interface* 2014;11: 20131146.
- [9] Kidder J F, Rouleau D, Pons-Villanueva J, Dynamidis S, DeFranco M, Walch G. Humeral head posterior subluxation on CT scan: validation and comparison of 2 methods of measurement. *Tech Should Surg* 2010;11: 72-76.
- [10] Frich, Lars Christian Jensen, Niels Odgaard, Anders Møger Pedersen, Claus Ole Søjbjerg, Jens Dalstra, Michel. Bone strength and material properties of the glenoid. *J Shoulder Elbow Surg / ASES ... [et al.]*. 1997. 6. 97-104. 10.1016/S1058-2746(97)90029-X.
- [11] Kalouche I, Crépin J, Abdelmoumen S, Mitton D, Guillot G, Gagey O. Mechanical properties of glenoid cancellous bone. *Clinical Biomechanics*. 2010, Volume 25, Issue 4, pages 292-298.
- [12] Gruetter R. (2018). *Fundamentals of biomedical imaging* (Lesson 4). Lausanne : EPFL, Ecole Polytechnique de Lausanne.
- [13] ASTM F2028-17, "Standard Test Methods for Dynamic Evaluation of Glenoid Loosening or Disassociation", ASTM International, West Conshohocken, PA, 2017, DOI:10.1520/F2028-17, [www.astm.org](http://www.astm.org)
- [14] Gérard Guell Bartrina, "Sensitivity analysis of a patient specific finite element model for shoulder arthroplasty", Laboratory semester project, under the supervision of Yasmine Boulanaache and Dr Alexander Terrier, Lausanne, Ecole polytechnique fédérale de Lausanne, 2017, 29 p.

- [15] Sandro Bergamin, "Overcorrected glenoid implants to avoid recurrent subluxation after total shoulder arthroplasty: a patient-specific finite element analysis". Master's thesis, under the supervision of Yasmine Meharzi, Dr Alexandre Terrier and Prof Dr Stephen Ferguson, Lausanne, Ecole polytechnique fédérale de Lausanne, 2017, 41 p.